HHS Public Access

Author manuscript

J Mater Chem B. Author manuscript; available in PMC 2021 December 21.

Published in final edited form as:

J Mater Chem B. 2020 December 21; 8(47): 10797–10811. doi:10.1039/d0tb02058c.

Development of an antibacterial and anti-metalloproteinase dental adhesive for long-lasting resin composite restorations

Eliseu A. Münchow[1,*], **Adriana F. da Silva**[2], **Evandro Piva**[2], **Carlos E. Cuevas-Suárez**[3], **Maria T. P. de Albuquerque**[4], **Rodolfo Pinal**[5], **Richard L. Gregory**[6], **Lorenzo Breschi**[7], **Marco C. Bottino**[8,*]

[1]Department of Conservative Dentistry, School of Dentistry, Federal University of Rio Grande do Sul, Porto Alegre, RS 90035-003, Brazil.

[2]Graduate Program in Dentistry, Federal University of Pelotas, Pelotas, RS 96015-560, Brazil.

[3]Dental Materials Laboratory, Academic Area of Dentistry, Autonomous University of Hidalgo State, Circuito Ex Hacienda La Concepción S/N, San Agustín Tlaxiaca, Hgo, 42160 Mexico.

[4]Department of Clinical Dentistry, Endodontics, Federal University of Bahia, Salvador, BA 40110-040, Brazil.

[5]Department of Industrial and Physical Pharmacy, Purdue University, College of Pharmacy, West Lafayette, IN 47907, USA.

[6]Department of Biomedical and Applied Sciences, Division of Dental Biomaterials, Indiana University School of Dentistry (IUSD), Indianapolis, IN 46202, USA.

[7]Department of Biomedical and Neuromotor Sciences, DIBINEM, University of Bologna, Alma Mater Studiorum, Bologna, Italy.

[8]Department of Cariology, Restorative Sciences, and Endodontics, University of Michigan School of Dentistry, Ann Arbor, MI 48109, USA.

Abstract

Despite all the advances in adhesive dentistry, dental bonds are still fragile due to degradation events that start during application of adhesive agents and the inherent hydrolysis of resin-dentin bonds. Here, we combined two outstanding processing methods (electrospinning and cryomilling) to obtain bioactive (antimicrobial and anti-metalloproteinase) fiber-based fillers containing a potent matrix metalloproteinase (MMP) inhibitor (doxycycline, DOX). Poly(ε)caprolactone

[*]**Co-corresponding authors:Eliseu A. Münchow, DDS, MSc, PhD**, Federal University of Rio Grande do Sul, School of Dentistry, Department of Conservative Dentistry, Porto Alegre, RS - 90035-003, Brazil, eliseumunchow@gmail.com (Dr. Eliseu A. Münchow), **Marco C. Bottino, DDS, MSc, PhD, FADM**, University of Michigan School of Dentistry, Department of Cariology, Restorative Sciences, and Endodontics, Ann Arbor, MI - 48109, United States, mbottino@umich.edu (Dr. Marco C. Bottino).

Author contributions

EAM and MCB conceived the original idea. AFS, EV and MCB designed the study and supervised the work. EAM synthesized the fibers and performed the experimental characterization of the fibers. EAM and RP fabricated the polymeric fillers derived from the electrospun fibers via cryomilling. MTPA and RLG performed the antibacterial analyses of the study. CECS and AFS performed experiments on gelatin zymography and nanoleakage challenges. EP assisted on statistical analyses. EAM tested the physico-mechanical properties of the fiber-modified adhesive resins, and wrote the article. LB gave technical advices regarding biological tests. LB and MCB critically revised the article.

Conflicts of interest

The authors declare no conflict of interest.

solutions containing different DOX amounts (0, 5, 25, and 50 wt.%) were processed via electrospinning, resulting in non-toxic submicron fibers with antimicrobial activity against *Streptococcus mutans* and *Lactobacillus*. The fibers were embedded in a resin blend, light-cured, and cryomilled for the preparation of fiber-containing fillers, which were investigated with antibacterial and *in situ* gelatin zymography analyzes. The fillers containing 0, 25, and 50 wt.% DOX-releasing fibers were added to aliquots of a two-step, etch-and-rinse dental adhesive system. Mechanical strength, hardness, degree of conversion (DC), water sorption and solubility, bond strength to dentin, and nanoleakage analyses were performed to characterize the physico-mechanical, biological, and bonding properties of the modified adhesives. Statistical analyses (ANOVA; Kruskal-Wallis) were used when appropriate to analyze the data (α=0.05). DOX-releasing fibers were successfully obtained, showing proper morphological architecture, cytocompatibility, drug release ability, slow degradation profile, and antibacterial activity. Reduced metalloproteinases (MMP-2 and MMP-9) activity was observed only for the DOX-containing fillers, which have also demonstrated antibacterial properties against tested bacteria. Adhesive resins modified with DOX-containing fillers demonstrated greater DC and similar mechanical properties as compared to the fiber-free adhesive (unfilled control). Concerning bonding performance to dentin, the experimental adhesives showed similar immediate bond strengths to the control. After 12 months of water storage, the fiber-modified adhesives (except the group consisting of 50 wt.% DOX-loaded fillers) demonstrated stable bonds to dentin. Nanoleakage was similar among all groups investigated. DOX-releasing fibers showed promising application in developing novel dentin adhesives with potential therapeutic properties and MMP inhibition ability; antibacterial activity against relevant oral pathogens, without jeopardizing the physico-mechanical characteristics; and bonding performance of the adhesive.

Graphical Abstract

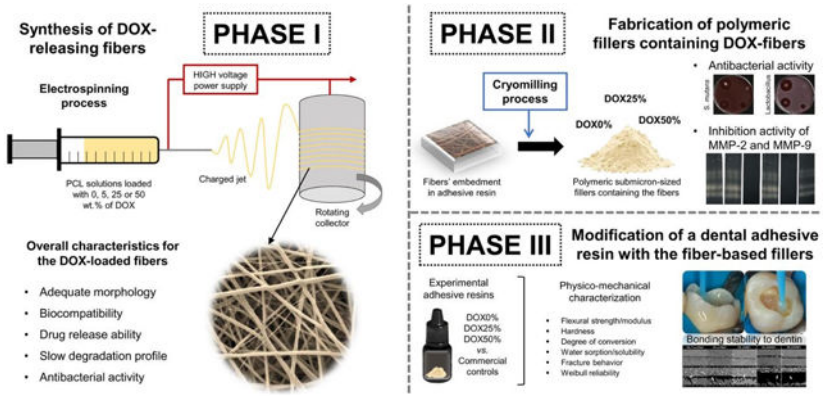

DOX-releasing fibers showed promising application in developing adhesives with therapeutic properties, i.e., matrix metalloproteinases inhibition ability and antibacterial activity.

Keywords

Doxycycline; Metalloproteinases; Polycaprolactone; Electrospinning; Dental Adhesives

1. Introduction

Success in adhesive dentistry means long-lasting resin composite restorations. Notwithstanding, the loss of adhesion or the retention of resin-based restorations (e.g., resin composites) is a frequent problem observed by dental practitioners, especially due to bond strength degradation.[1] According to the literature,[2,3] degradation of resin-dentin interfaces may occur within the collagen fibrils at even earlier stages (e.g., immediately after application of bonding agents), but also after polymerization of the adhesive material (material degradation). While the former involves activation of bound matrix metalloproteinases (MMPs), which are enzymes that slowly degrade collagen fibrils exposed during acid etching of the substrate,[4] the latter involves degradation of hydrolytically susceptible groups (e.g., ester, urethane, hydroxyl, carboxyl, phosphate) found in the molecular structure of methacrylate-based resin monomers.[5,6]

Researchers have focused on evaluating strategies that would improve the stability of resin-dentin bonds over time. Some approaches involve the use of chemical agents, including but not limited to collagen cross-linkers, antioxidants, MMP inhibitors, and remineralizing agents; whereas, other strategies are focused on modification of the bonding procedure itself or the physical treatment of dental substrates prior to application of the bonding agents.[7] Among the foregoing strategies, the use of MMP inhibitors raises the interest of clinicians, probably due to the interruption of collagen degradation in the case of bound MMPs being activated. There are several MMP inhibitors used in dentistry for that purpose, such as chlorhexidine (CHX), metallic monomers, and some tetracycline-derived agents, such as doxycycline (DOX).[7–9]

DOX is a potent MMP inhibitor able to chelate calcium and zinc ions, hampering the maintenance of structural and functional active sites of the enzyme, resulting in MMP inactivation.[10–14] However, the incorporation of DOX into a low-viscous resinous adhesive may impair bonding performance due to phase separation reactions that can possibly occur.[15] Notably, DOX has been successfully incorporated into dental adhesives via their encapsulation into nanotubes, resulting in both the inhibition of MMP and adhesive stability.[10] Despite its effectiveness, it is well-established that the incorporation of nanotubes into dental materials is commonly minimal (e.g., up to 1 wt.%), since there is a maximum concentration threshold involved; otherwise, the material may significantly change color (e.g., become greyish),[16] which may affect the acquisition of adequate polymerization.[17] Alternately, polymeric nanofibers obtained via electrospinning have been broadly used as stable vehicles for the release of bioactive compounds, such as DOX,[18] thus holding enormous potential in adhesive dentistry. Nevertheless, and to the best of our knowledge, the specific modification of a dental adhesive resin with electrospun fibers has never before been attempted.

Despite it being an interesting approach, there is one special concern regarding the incorporation of electrospun fibers into dental adhesives, i.e., the high-surface energy of small-sized fibers makes their incorporation and effective dispersion difficult without causing phase separation reactions and/or physical instability of the mixture.[19] Altogether, the present study proposed a distinct method of accomplishing this goal: further processing

the electrospun fibers into a powder/filler via cryomilling, as demonstrated elsewhere,[20] facilitating homogeneous incorporation of the bioactive fibers into the adhesive resin. Hence, this study aimed to synthesize DOX-releasing electrospun fibers, which were further processed into submicron-sized fillers, and investigate their effects on physico-mechanical and biological properties, as well as on bonding performance to dentin of a fiber-modified two-step, etch-and-rinse dental adhesive system.

2. Experimental

This study was carried out in three phases. First, DOX-releasing polymeric fibers were synthesized via electrospinning and characterized with morphological, biocompatibility, drug release, degradation *in vitro*, and antimicrobial analyzes. Second, submicron-sized fillers were obtained from DOX-releasing fibers via cryomilling and they were tested by means of antimicrobial and *in situ* zymographic analyses. Last, a commercial dental adhesive system was modified with the fiber-containing fillers and evaluated with selected physico-mechanical analyses, immediate and long-term bonding performance to dentin, and nanoleakage challenge.

2.1. Phase I

2.1.1. Synthesis of DOX-releasing polymeric fibers—Poly(ε-caprolactone) pellets (PCL, Sigma-Aldrich, St. Louis, MO, USA) were dissolved in 1,1,1,3,3,3-hexafluoro-2-propanol (HFP, Sigma-Aldrich) to produce a 10 wt.% polymer solution (100 mg mL^{-1}). After overnight stirring, doxycycline (DOX, Sigma-Aldrich) was added at different concentrations (0, 5, 25, and 50 wt.%, relative to the total polymer weight); the mixtures were stirred for 24 h. The solutions were electrospun using an electrospinning system consisting of a high-voltage source (ES50P-10W/DAM, Gamma High-Voltage Research, Inc., Ormond Beach, FL, USA), a syringe pump (Legato 20, KD Scientific Inc., Holliston, MA, USA), and a grounded stainless steel collecting drum connected to a high-speed mechanical stirrer (BDC6015, Caframo Limited, Georgian Bluffs, ON, Canada). Each solution was loaded into a plastic syringe (5 mL, Becton, Dickson and Company, Franklin Lakes, NJ, USA) fitted with a 27G metallic blunt-tip (CML Supply LLC, Lexington, KY, USA) and electrospun using the following parameters: rotating mandrel (120 rpm of speed), fixed spinning distance of 18 cm, flow rate of 1.5 mL/h, and electric voltage of 15 kV. The obtained fiber mats were collected at room temperature and dried under vacuum for at least 48 h to complete removal of any remaining solvent.[21,22]

2.1.2. Characterization of the electrospun DOX-releasing polymeric fibers—For morphological characterization, the fiber mats were observed under a field-emission scanning electron microscope (FE-SEM, Model JSM-6701F, JEOL, Tokyo, Japan). Samples taken from each mat were mounted on Al stubs and sputter-coated with Au-Pd prior to imaging. ImageJ software (National Institutes of Health, Bethesda, MD, USA) was used to calculate the diameter of 50 single-fibers per image obtained from the FE-SEM analyses (3 images/group) at the same magnification (5000×); the fiber diameter was then averaged and reported as mean ± SD.[21]

For cytocompatibility analysis, the guidelines provided by the International Standards Organization/ISO[23] were followed in order to detect toxicity levels of the processed fibers.[24] Human dental pulp stem cells (hDPSCs, AllCells, LLC, Alameda, CA, USA) obtained from permanent third molars were cultured in low glucose Dulbecco's Modified Eagle's Medium (DMEM, Gibco, Invitrogen Corporation, Grand Island, NY, USA) supplemented with 10% FBS (Hyclone Laboratories, Inc., Logan, UT, USA) and 1% penicillin–streptomycin (Sigma-Aldrich) in a humidifier incubator at 37°C, with 5% CO_2. Extracts from each mat were prepared by incubating sterile samples (15 mm × 15 mm, surface ratio = 1 cm^2/mL of medium) in DMEM for 48 h at 37°C under a 5% CO_2 humidified atmosphere; extracts of sterile ultra-high molecular weight polyethylene (UHMWPE) were similarly obtained (negative control). Supernatants were then filtered through a membrane (Millipore®, MilliporeSigma, Burlington, MA, USA), and serial dilutions (100, 50, 25, 12.5, and 6.25 vol.%) were prepared from the extracts. Dilutions were also performed for the positive control (i.e., 0.3 vol.% phenol solution). hDPSCs were seeded at a density of 3×10^3/well and allowed to adhere in the wells of 96-well tissue culture microtiter plates. Control columns of four wells were prepared with a medium without cells (blank), and a medium with cells but without the extract (100% survival). The microplate was incubated again, and after 48 h, the amount of 20 μL of CellTiter 96 AQueous One Solution Reagent (Promega Corporation, Madison, WI, USA) was added to the test wells and allowed to react for 2 h at 37°C in a humidified 5% CO_2 atmosphere. The incorporated dye was measured by reading the absorbance at 490 nm in a microplate reader against a blank column.

Evaluation of the drug release from the DOX-loaded fiber mats (15 × 15 mm^2, n=4) was done via high-performance liquid chromatography (HPLC), as demonstrated elsewhere.[25] The fiber mats were weighed and then immersed in PBS (10 mL) for 28 days. The aliquots (1 mL) were removed from each solution at selected time points (1, 3, 7, 14, and 28 days) and replaced with an equal amount of fresh PBS at each collection. They (10 μL) were analyzed using HPLC-UV equipment (Agilent 1100 System, Agilent Technologies Inc., Palo Alto, CA, USA; Zorbax SB-phenyl chromatography column), which consisted of a binary mobile phase of solvent systems A (0.1% formic acid in ddH_2O, v/v) and B (0.1% formic acid in acetonitrile, v/v) in a gradient elution. Test parameters were described in detail elsewhere.[24] The percentage of the released drugs was then calculated on the basis of the initial weight of the fiber mats.

For *in vitro* degradation of the fiber mats, samples (15 × 15 mm^2, n=4) of each group were soaked in a vial filled with 50 mL of PBS buffer (pH=7.4) for 90 days at 37°C. The PBS solution was replaced by fresh PBS every two weeks. The fiber mats were then gently removed, air-dried, mounted on Al stubs, sputter-coated with Au-Pd, and observed under FE-SEM. The fiber diameter was calculated as aforementioned.

The antibacterial activity of the processed fibers was evaluated against *Streptococcus mutans* and *Lactobacillus* using agar diffusion assays (n=3/group/bacteria).[26] Briefly, the bacteria were cultivated in Brain Heart Infusion (BHI) broth supplemented with 5 g yeast extract/L and 5% (v/v) vitamin K+hemin at 37°C. Disk-shaped samples (5-mm in diameter) were prepared and sterilized through ultraviolet (UV) irradiation for 1 h (30 min each side),

before placing on culture blood agar plates, as previously indicated.[22] The inhibition zone (in mm) of each sample was measured at days 1, 3, 7, 14, and 28.

2.2. Phase II

2.2.1. Preparation of fiber-containing polymeric fillers—Fiber-containing fillers were fabricated, as demonstrated elsewhere.[20] To that end, the fiber mats were cut into pieces (30 × 30 mm^2) and immersed into a resin blend composed of 60 wt.% bisphenol glycidyl A methacrylate (Bis-GMA), 40 wt.% 2-hydroxyehtyl methacrylate (HEMA), and 0.4/0.8 wt.% of CQ/DMAEMA (initiation system). All monomers and initiators were purchased from Sigma-Aldrich. Each soaked piece was then cautiously removed and placed in-between two Mylar sheets and two glass plates. Light finger pressure was applied to remove any excess resin and air bubbles. The samples were light-cured for 2 min on each side in a TRIAD 2000 chamber (Dentsply Sirona Inc., York, PA, USA), resulting in resin/mat composites with a fiber content of approximately 25 wt.%. Next, all the resin/mat composites were subjected to a cryomilling process using a cryogenic impact mill (model SPEX CertiPrep 6750, SPEX CertiPrep, Metuchen, NJ, USA) to obtain a fine submicron-sized powder. The samples were precooled for 2 min and then milled for 15 min, which consisted of alternating cycles of 1 min of milling time separated by 1 min cooling intervals. Liquid nitrogen surrounding the milling chamber was used to ensure complete cooling during cycles.

2.2.2. Characterization of the fiber-containing fillers—The fillers were suspended in PBS (10 mg/mL) and stirred overnight for proper dispersion; they were then tested against *S. mutans* and *Lactobacillus* bacteria using agar diffusion assays, as described previously. Twenty μL of each suspension was pipetted on blood agar plates and the inhibition zones (in mm) of each sample were measured at days 1, 4, and 12. CHX was used as the control.

The fillers were also evaluated for the inhibition potential of MMP activity via gelatin zymography testing. MMPs were obtained from the saliva of donors following approval by the local Ethics Committee (protocol 2.078.368/2017). Briefly, the saliva containing MMPs were centrifuged and frozen at −80°C. Enzyme purification (72-kDa [MMP-2] and 92 k-Da [MMP-9] type IV collagenases) was performed according to the modified protocol described by Chen et al.[27] After thawing, the protein concentration was determined by a Bio-Rad Protein Assay (Bio-Rad Laboratories, Inc., Hercules, CA, USA) using the Bradford method. Fifteen ng of each sample was mixed with non-reducing buffer (2% SDS; 125 mM Tris-HCl, pH 6.8, 10% glycerol; and 0.001% bromophenol blue). The resulting media were loaded in 10% sodium dodecyl sulfate-polyacrylamide gels copolymerized with 1.6 mg/mL of gelatin (Sigma-Aldrich) as substrate. Protein renaturation was performed by incubation of the gels in 2% Triton X-100 (Sigma-Aldrich), and then the gels were split and loaded into 1-cm strips, which were individually incubated in 50 mL of conditioned activation buffer (50 mM Tris-HCl, pH 7.4, 5 mM $CaCl_2$) for 16 h at 37°C. The gels were all incubated into each of the following experimental conditions: eluates obtained from the fiber-containing fillers loaded with 0, 25, and 50 wt.% of DOX-releasing fibers; 0.5 mM of NEM (N-ethyl-maleimide; positive control); 0.5 mM of EDTA (ethylenediaminetetraacetic acid; negative control); and 0.5 mM of Tris–$CaCl_2$ buffer (control – standard reference).[28] After addition of

the eluates to the solution, the pH was adjusted to 7.4 and incubated at 37°C for different periods (6 h and 7 days) in 50 mM Tris–HCl buffer containing 5 mM $CaCl_2$ (Tris–$CaCl_2$). After incubation, the gels were stained with 0.05% Coomassie Brilliant Blue G-250, and the gelatinolytic activity was visualized as clear bands against the blue background on stained gels. Each assay was performed in triplicate and repeated at least twice.[28]

In light of quantifying the relative enzyme activity, the bands related to the proactive and active forms of MMPs 2 and 9 were digitalized and the images analyzed using ImageJ software. To that end, the images were converted to grayscale and the background was subtracted in order to prevent the influence effect in the density of the pixels. The density of each band was calculated three times and the values were averaged. The enzymatic activity of the standard control group was taken as 100% of activity, and the percentage increase or decrease in enzymatic activity of the other groups was then calculated using that reference. Increased values were indicative of greater enzyme activity, whereas reduced values represented inhibition effects on the MMPs.[29]

2.3. Phase III

2.3.1. Modification of a dental adhesive with fiber-containing fillers—

Fiber-containing fillers with a DOX level of 25 and 50 wt.% or without DOX (DOX0%) were added into aliquots of a two-step, etch-and-rinse dental adhesive system (One-Step®, BISCO Dental Products, Schaumburg, IL, USA), which is an unfilled resin adhesive. The fillers were added (20 wt.%) without prior functionalization (surface treatment);[30] one aliquot of the adhesive was kept unmodified to serve as an unfilled control (OS). A commercial adhesive system containing inorganic filler particles was also used in this study as an additional control (One-Step® Plus, BISCO Dental Products), serving as a filled version material (OS_Plus). The experimental fiber-modified adhesives were stirred for 15 min in dark conditions in an attempt to allow the dispersion of fillers and adequate mixture to the resin matrix.

2.3.2. Physico-mechanical characterization of the fiber-modified adhesives—

The fiber-modified adhesives, as well as the unfilled control, were tested with the following analyses: flexural strength, flexural modulus, hardness, degree of conversion, and water sorption and solubility. For flexural strength (σ) and flexural modulus (E), bar-shaped specimens (25 mm long × 2 mm wide × 2 mm thick, n=10) were prepared for each group according to ISO 4049.[31] Each specimen was light-cured for 25 s in four overlapping irradiation zones on both the top and bottom surfaces. The specimens were stored in distilled water at 37°C for 24 h, and then submitted to the three-point bending test (MTS Sintech ReNew 1123, MTS Systems Corporation, Eden Prairie, MN, USA) at a crosshead speed of 1 mm/min. The σ and E were calculated using the following equations and expressed in MPa and GPa, respectively:

$$\sigma = \frac{3Fl}{2bh^2} \quad E = \frac{3F1l^3}{4bh^3d}$$

where F is the load at fracture (N), l is the distance between supports (20 mm), b is the width of the specimen (mm), h is the thickness of the specimen (mm), $F1$ is the maximum load in the linear portion of the load-displacement curve, and d is the deflection of the specimen at load $F1$. Representative samples from the fractured specimens were also selected and evaluated for SEM analysis. The samples were dried and the fractured surfaces were sputter-coated with Au-Pd and observed under FE-SEM. Fractography principles were applied for the qualitative analysis of the micrographs.[32]

For hardness analysis, the fractured specimens derived from mechanical testing were subjected to microhardness testing (M-400, LECO Corporation, St. Joseph, MI, USA) using a Knoop diamond indenter, 50 kg of load, and 15 s of dwell time. Five readings with a minimum of 100 microns between indentations were obtained from each specimen. The diagonal lengths were measured immediately after each indentation, and the values were converted to Knoop hardness number (KHN).

The degree of conversion (DC) was evaluated using a Fourier Transform infrared spectrometer (model 4100, JASCO International Co., Ltd., Tokyo, Japan) equipped with an attenuated total reflection device in the absorbance mode (8 cm^{-1} resolution and 2.8 mm/s mirror speed). Uncured specimens (6 mm in diameter × 0.25 mm thick, n=3) were prepared and measured, followed by their light-activation for 25 s using a light-emitting diode light-curing system (DEMI LED, Kerr Corporation, Orange, CA, USA), and they were then measured again (cured state). The light irradiance was >900 mW/cm^2. The absorbance bands at 1637 cm^{-1} (methacrylate group, C=C) and 1607 cm^{-1} (ester group, C=O) were used to calculate the DC (expressed in %) using the following equation:

$$DC = 1 - \frac{cured\left(\text{area under 1637}\quad cm^{-1}/\text{area under 1607}\quad cm^{-1}\right)}{uncured\left(\text{area under 1637}\quad cm^{-1}/area\ under\ 1607\quad cm^{-1}\right)} \times 100\%$$

For water sorption and solubility analysis, ten disk-shaped specimens (6 mm diameter × 1 mm thick) were prepared according to ISO 4049,[31] except for the dimensions of the specimen.[33] The specimens were placed into a desiccator containing freshly dried silica gel and calcium chloride. After 24 h, the mass of each sample was measured daily using a precision balance of 0.01 mg of readability (AUW 220D, Shimadzu Corporation, Nakagyo-ku, Kyoto, Japan) until a constant mass (m_1) was obtained. The thickness and diameter of the specimens were randomly measured at five points using a digital caliper to calculate their volume (V, in mm^3). The specimens were immersed in distilled water at 37°C for 7 d, blot-dried, and weighed (m_2). After weighing, the specimens were dried again inside the desiccator and weighed daily to record a third constant mass (m_3), as previously described. The water sorption (WS) and solubility (SL) of each specimen was calculated in μg/mm^3, using the following equations:

$$WS = \frac{m_2 - m_3}{V} \quad SL = \frac{m_1 - m_3}{V}$$

2.3.3. Bonding performance and fracture analysis of the fiber-modified adhesives—Forty freshly extracted sound human molars were selected following approval by the local Ethics Committee (protocol 2.078.368/2017). The teeth were first stored in 0.5% chloramine T solution for 7 d, then stored in distilled water until use. The occlusal enamel was sectioned perpendicular to the long axis of the tooth in a low-speed diamond saw machine (Isomet 1000, Buehler Ltd., Lake Bluff, IL, USA) to expose the subjacent dentin that was wet ground flat with 600-grit silicon carbide (SiC) abrasive paper until a uniform enamel-free dentin surface was obtained. The root of each tooth was removed about 2-mm above the cementum-enamel junction using the saw machine parallel to the occlusal surface, as previously described. The samples were randomly allocated into five groups (n=8) according to the adhesive system applied: the filled control adhesive (OS_Plus), the unfilled control adhesive (OS), and the fiber-modified adhesives (OS_DOX0%, OS_DOX25%, and OS_DOX50%). All the adhesive resins were applied to the tooth samples following the directions for use by the commercial controls. Briefly, the entire dentin surface was etched with 37% phosphoric acid gel (Condac 37; FGM, Joinville, SC, Brazil) for 15 s and rinsed with distilled water for 15 s. The dentin surfaces were dried with a gentle stream of oil-free compressed air for 5 s, from a distance of 10 cm, leaving the surface visibly moist. The fiber-modified adhesives were all sonicated for 15 min before use; the filled control adhesive was manually agitated (manufacturer's directions for use). The adhesives were then applied with a disposable brush and agitated slightly for 15 s; two coats of each respective adhesive were used for bonding to each tooth sample. The solvent was evaporated using a gentle stream of air until a shiny surface was obtained, and light-activation was performed with the LED for 25 s. Next, two increments of a nanofilled resin composite (Filtek™ Z350, 3M ESPE, St. Paul, MN, USA), nearly 2 mm-thick, which completely covered the dentin surface, were light-activated for 25 s each and placed. The samples were stored in distilled water at 37°C for 24 h.

All the samples were sectioned in two directions perpendicular to the bonded interface using the foregoing saw machine at low-speed, resulting in resin-dentin specimens with a cross-sectional surface area of approximately 0.8 mm^2 for microtensile bond testing. The specimens were randomly allocated according to the storage period: immediate testing (24 h) and long-term testing (12 months of distilled water storage at 37°C). For immediate and long-term testing, the extremities of each microtensile specimen were individually fixed to a custom-made testing jig with a cyanoacrylate glue (Super Bonder Gel, Loctite, Henkel AG & Company, KGaA, Düsseldorf, Germany) and tested in a mechanical testing machine (DL-500, Instron Brazil Scientific Equipment Ltd., Sao Jose dos Pinhais-PR, Brazil) at a crosshead speed of 1 mm/min until failure. The microtensile bond strengths (μTBS) were calculated and expressed in MPa. The fractured specimens were examined under a stereoscopic loupe at 40× magnification. The failure pattern was classified as follows: adhesive, cohesive in dentin, cohesive in resin composite, and mixed (i.e., more than one of the foregoing failure modes).

2.3.4. Nanoleakage challenge—Three resin-dentin specimens obtained during immediate bond strength testing from each group were randomly chosen and used for nanoleakage evaluation.[34] The specimens were placed in an ammoniacal silver nitrate

solution in darkness for 24 h, rinsed thoroughly in distilled water, and immersed in photo-developing solution for 8 h under a fluorescent light. The specimens were rinsed with distilled water, air dried and placed inside a PVC ring attached to a double-sided adhesive tape, and embedded in epoxy resin (Fiberglass Commercial, Porto Alegre, RS, Brazil). After setting, the embedded specimens were reduced to approximately half of their thickness by grinding with 400-grit SiC papers under running water. The specimens were then polished with wet 1000-, 1200-, and 2000-grit SiC papers and 3 μm and 1 μm diamond paste (Buehler). They were ultrasonically cleaned, air-dried, and coated with gold for SEM evaluation operated in the backscattered mode (JSM-6610LV, JEOL).

2.4. Statistical analysis

The data obtained in this study were analyzed with SigmaPlot (version 12; Systat Software, Inc., San Jose, CA, USA) using Analysis of Variance (one-way for cell viability, mechanical properties, hardness, degree of conversion, and water sorption; or two-way for antibacterial activity, percentage MMP activity, and bond strength to dentin). The Kruskal-Wallis test was used to analyze data on fiber diameter (before and after PBS storage) and water solubility. The Tukey and Student-Newman-Keuls *post hoc* tests were used to analyze parametric and non-parametric data, respectively. The level of significance was set at $\alpha=0.05$ for all analyses. The reliability and probability of failure of the unmodified and fiber-modified adhesive resins were analyzed by Weibull analysis with a 95% confidence interval.[35]

3. Results and discussion

3.1. Characterization of the DOX-releasing fibers

Electrospun fibers containing DOX at 5, 25, and 50 wt.% were successfully obtained, since they demonstrated satisfactory morphology, cytocompatibility, drug release ability, slow degradation profile, and significant antimicrobial activity against prevalent oral bacterial species. Morphological analysis revealed that the presence of DOX contributed to the fabrication of fibers with a narrower diameter distribution (Gaussian) as compared to the DOX-free counterparts (Figure 1). The median fiber diameter for all groups decreased in the following order: DOX25% (296.3 nm [58.2 – 672.0 nm]) > DOX5% (264.6 nm [164.0 – 550.3 nm]) = DOX50% (264.6 nm [31.7 – 608.5 nm]) > DOX0% = (187.8 nm [58.2 – 1582.0 nm]). All DOX-containing fibers exhibited greater median values than the DOX0% group ($p<0.001$). Despite their thinner morphology, the DOX0% fibers demonstrated the most heterogeneous diameter distribution of the study. One may suggest that the hydrophilicity of DOX (i.e., its molecular structure, possesses five polar hydroxyls) reduced chain entanglement of the hydrophobic PCL solution during electrospinning, resulting in more homogeneous, standardized fibers.[36] This effect was corroborated by other studies that also incorporated hydrophilic substances, such as DOX into electrospun polymeric fibers.[37–39] Remarkably, all the obtained fibers were randomly oriented, smooth, and free of beads, denoting the adequate electrospinning parameters used and the concentration balance between the polymer solution and DOX.[40]

Another essential aspect for any fiber-based structure is the biological safety to human tissues; otherwise, its clinical application would probably pose a health risk to the

individual. The present fibers were all non-toxic (cell viability > 70%),[23] regardless of DOX concentration (Figure 2A). However, the fibers containing 50 wt.% DOX demonstrated lower cell viability compared to the other groups ($p \leq 0.031$), which showed similar biocompatibility to the UHMPE negative control ($p \geq 0.056$). Conversely, phenol solution (positive control) resulted in cytotoxic behavior. A previous study by Wittrig et al.[41] reported that cell proliferation increased in the presence of a tetracycline, and considering that DOX is a tetracycline-derived substance, a biocompatible behavior could be expected in our study. Also, Trajano et al.[42] demonstrated that a composite containing 25 μg/mL of DOX (i.e., similar to the DOX25% fiber mats) induced greater osteoblast proliferation as compared to the composite material without DOX (control), indicating the excellent bioactivity of this compound upon this appropriate concentration level. No less important, different extract concentrations were tested in our study in order to verify whether greater amounts of DOX would account for a less biocompatible behavior; nevertheless, even the most concentrated extracts demonstrated good cell compatibility.

Concerning the drug release profile of fibers, Figure 2B reveals a burst release of DOX within the first 24 h, which was sustained for the DOX50% group but not for those less concentrated, which displayed a progressive concentration reduction throughout 3 (DOX5%) and 7 days (DOX25%) of incubation. One possible explanation related to this different release profile relies on the fact that the greater the amount of DOX, the higher the presence of hydroxyls within the fiber, contributing to the formation of hydrogen bonding and intermolecular interactions,[43] and to the decreased release rate of the DOX50% group. Other studies also suggested that the lower the content of the bioactive ingredient, the lower its incorporation into the polymer matrix, thus resulting in its faster release.[38,44] Indeed, it seems that DOX was accumulated near the surface of the fibers, resulting in an isotropic degradation mechanism that relates to a burst release profile of the drug.[45] Moreover, the electrospun fibers synthesized here were all randomly oriented, and according to the study by Eslamian et al.,[45] poorly aligned fibers may present burst and less sustained release of DOX when compared to fibers with highly alignment orientation.

Electrospun fibers are expected to degrade at a certain level in order to act as a well-controlled carrier vehicle. From several polymer sources available for electrospinning, PCL is a biodegradable thermoplastic polymer that presents relatively low-cost and good spinnability; therefore, it was chosen in our study.[46] The neat PCL fibers prepared without DOX suffered the strongest degradation after PBS storage for 90 days, resulting in considerable morphological changes (Figure 3). Different from the original fibers, the DOX0% fibers became approximately 4 times thicker ($p < 0.001$) and acquired a flattened architecture, clearly indicating the relaxation process derived from liquid uptake.[47] Surprisingly, the DOX-containing fibers did not degrade in the same fashion as the neat fibers, maintaining the fiber diameter distribution similar to their original shape ($p > 0.05$). Here, it may be suggested that DOX somewhat improved the polymeric network of the PCL fibers, probably related to the formation of hydrogen bonding as discussed previously, thus improving the fibers' resistance to the relaxation phenomena of degradation. One may also suggest that the presence of DOX at high levels (50 wt.%) improved the crystalline nature of the PCL fibers, resulting in the release of DOX being slightly more sustained than that of the less concentrated groups.[48] The idea that DOX improved the crystalline structure of the

fibers, regardless of concentration, may have contributed to the dimensional and physical stability of the DOX-loaded fibers. This effect could be interestingly applied to the development of fibers with a much slower degradation rate as compared to other typical polymer formulations (e.g., gelatin-based blends), which tend to degrade following a faster scenario. In dentistry, this would contribute to the long-lasting application of the fibers, warranting further investigation, perhaps aiming for alternative goals, such as the strengthening of dental restoratives.

As shown in Table 1, all DOX-releasing fibers demonstrated antimicrobial activity against *S. mutans* and *Lactobacillus* for at least 7 days of storage, which is in accordance with the considerable fast DOX release profile shown by the fibers, corroborating the findings of similar studies.[38,39,49] The antibacterial mechanism of DOX is the same for any tetracycline-derived substance, which means it inhibits the cleavage and processing of bacterial rRNA transcripts/precursors, leading to the impaired formation of mature rRNAs and the consequent inhibition of protein synthesis,[50] i.e., bacterial death. During the initial days of incubation, DOX25% and DOX50% fibers exhibited greater antibacterial activity compared to CHX (control) and DOX5% fibers ($p<0.05$) losing their antibacterial effects between 7 and 14 days. Conversely, CHX sustained its antibacterial property for longer periods. CHX is a potent organic antimicrobial agent with low cytotoxicity to soft tissues,[51] and it is a cationic biguanide that adsorbs onto the cell wall of microorganisms and causes leakage of intracellular components, showing effectiveness against both Gram-positive and Gram-negative bacteria.[52] The substantivity of CHX is already well-recognized in the literature and, according to Khademi et al.,[53] its antimicrobial effects may last for far longer periods than DOX. In our study, *S. mutans* and *Lactobacillus* were selected, because they are both involved in the formation of cariogenic biofilms when dietary sucrose and starch are present,[54,55] and any positive effect of our fibers against these microorganisms would be interestingly used to modify dental materials that lack a caries prevention ability. Up to this point, the present DOX-releasing fibers demonstrated satisfactory performance by means of relevant morphological and biological characteristics.

3.2. Characterization of the fiber-containing fillers

Taking into consideration the appropriateness of the synthesized fibers, they were further processed into small-sized fillers in order to facilitate their incorporation into a dental adhesive system, since long fibers are difficult to properly embed into low viscous resin formulations. The processing used in our study was cryomilling, which consists of cooling a material, then reducing it to small-sized particles.[20,56] According to a similar study by Hamilton et al.,[20] which fabricated fiber-based polymeric fillers using the same method employed here, the originated fillers were found to be at the submicron scale, showing an irregular morphology and average size of 15 μm, resulting in the same pattern of fillers as expected here. One of the major concerns about transforming electrospun fibers into a powder/filler would be the loss of biological activity due to the cooling and/or mechanical processing. Notwithstanding, the obtained fillers derived from the DOX-releasing fibers maintained their antimicrobial activity against *S. mutans* and *Lactobacillus* (Figure 4), except for the fillers obtained from the less concentrated fibers (DOX5%; no inhibition zones); this latter group was no longer investigated in this study. It seems that the total

amount of the drug found in the original electrospun fibers, which was effective against the tested bacteria (Table 1), was significantly reduced after cryomilling, thereby decreasing the antibacterial potential for the DOX5% fillers. It may be inferred that DOX was probably released at a level below the minimum inhibition concentration or at a slower release rate,[57] losing effects against the bacteria. Nevertheless, the antibacterial properties of the more concentrated DOX25% and DOX50% fillers were maintained, resulting in greater inhibition zones than CHX, denoting their excellent bioactivity. It may be suggested that the fibers became shorter during cryomilling, with DOX being detached more easily from the fibers, which improved the availability of this substance within the resulting fillers.[20] Moreover, the surface area of small-sized fillers is expected to be greater in comparison to the fibers, and increase the bioavailability of DOX.[58]

Regarding the inhibition potential of MMPs' activity, both the fiber-containing fillers loaded with 25 and 50 wt.% DOX were effective in inhibiting MMP-2 and MMP-9 expression after 7 days of incubation (Figure 5), differing from the DOX-free fillers that have demonstrated no MMP inhibition potential. Endogenous MMP-2 and −9 are present in latent forms (inactives) in mature, sound, mineralized human teeth, but upon application of acidic substances (e.g., etch-and-rinse or self-etching adhesive systems), the MMPs acquire the active form, starting degradation of the collagen fibrils (dentin matrix).[59] One interesting aspect of our findings is that the inhibiting effect of the obtained fillers seemed to rely on both the concentration of DOX in the filler and the incubation period of the eluates. Of note, the DOX25% fillers allowed enzymatic activity at the 6 h period, showing a greater percentage activity (26–57%) than the standard control. Similarly, the DOX0% and positive control (NEM) also showed relatively increased activity compared to the standard Tris-$CaCl_2$ buffer, suggesting that a more suitable environment for gelatinolytic activity was achieved in the foregoing eluates. One may consider that some metabolic products (e.g., methacrylic acid) were released from hydrolysis of the polymeric content of the fillers during eluate preparation, creating an acidic environment and an increased MMP' expression.[29,60] Conversely, at the 7-day period, enzymatic activity significantly decreased for the DOX-containing fillers, probably due to an inhibitory effect of the MMPs. Here, we may suggest that time was necessary to reach a minimum amount of DOX released from the fillers, and once the availability of DOX was sufficient, the expression of the enzymes was reduced. In theory, DOX release had probably occurred following a sequential diffusion mechanism, starting with its diffusion from the shortened electrospun fibers, followed by its diffusion through the resin matrix of the fillers, thereby reaching the surface of each filler particle and becoming available for proper MMP inhibition.[61,62] One should consider that the polymeric fillers prepared in this study may have acted as microcarriers, which can be advantageous over the use of smaller carrier vehicles, such as nanoparticles/nanofibers, due to the longer-term release profile of the former, contributing to a sustained and well-controlled release of the active drug.[61] Also, according to Khalf et al.,[36] water uptake is necessary for the effective mobility and release of DOX within polymer networks, hence corroborating our findings. As a result, the DOX release profile seemed to occur following a much slower scenario in the fillers than for the fiber mat carriers, deserving further investigation.

Different from the DOX25% group, the DOX50% fillers resulted in the inhibition of MMP-2 and −9 at even the 6 h period, probably due to their greater content of DOX. The literature reveals that DOX inhibits MMP activity due to a chelating mechanism, since it prevents the binding of ions such as Zn^{+2} and Ca^{+2} to the MMPs structure, inhibiting the MMP catalytic activity.[7] According to the study by Jun et al.,[63] which tested the effects of copper(Cu)-doped bioactive glass nanoparticles on the deactivation of MMPs, the higher the content of Cu^{+2} ions released, the greater the reduction in MMP-degradation activity in demineralized dentin. As shown by our findings, the fillers containing DOX-releasing fibers were effective in the inhibition of MMPs 2 and 9, so that we may infer that the bonding agent modified with these fillers would prevent the activation of MMPs during the critical steps of bonding a restoration to the tooth (acid etching and priming, depending on the systems used). Last but not least, in our study, the MMPs were obtained from human saliva, since a previous study demonstrated the occurrence of significant amounts of MMPs in this oral fluid.[64] Of note, enzyme purification was performed accordingly and both negative and positive controls were used, confirming that our experimental fillers acted in the inhibition of activity of the tested MMPs. Other proteases, such as cathepsins and distinct MMPs, which are also responsible for dentin matrix degradation, should be tested in order to demonstrate whether our strategy of using DOX/fiber-based fillers would still be effective. Overall, the cryomilling process demonstrated here did not jeopardize the bioactivity of the DOX/fiber-releasing fillers, suggesting their suitability to improve the biological properties of dental adhesive systems.

3.3. Physico-mechanical characterization of the fiber-modified adhesives

The fiber-modified adhesives tested in our study were comprised of polymeric fillers structurally based on shortened electrospun fibers with or without DOX. Usually, electrospun fibers possess a tough and flexible behavior (e.g., high elongation at break) due to their very long, thin nature.[65] Nevertheless, this mechanical behavior was not expected to be translated to the fiber-modified adhesives, because the fibers were reduced in size and intrinsically embedded by the resin matrix of the fillers, and polymeric fillers are commonly associated with a significant decrease in strength properties.[30] Surprisingly, both the flexural strength and flexural modulus of the fiber-based adhesives were statistically similar, compared to the unfilled control ($p \geq 0.151$), as shown in Figure 6 (A–B). Hardness tended to decrease for the filled resin adhesives (Figure 6C), although only the group containing DOX50% fillers showed a significant hardness reduction compared to the control ($p=0.009$). The degree of conversion was statistically greater ($p<0.001$) for the DOX-modified adhesives (Figure 6D), although only a slight increment in the conversion of monomers was indeed observed; the fiber-based adhesive free of DOX showed a similar degree of conversion compared to the control ($p=0.057$). Concerning the physical stability of the resin adhesives after water storage, the DOX-modified adhesives showed similar water sorption as the control ($p \geq 0.058$); whereas, the OS_DOX0% adhesive exhibited the lowest water sorption of the study (Figure 6E). In terms of water solubility, the OS_DOX0% and OS_DOX25% groups demonstrated lower solubility than the control and the OS_DOX50% groups ($p<0.05$), which did not differ between each other (Figure 6F).

Overall, incorporation of the synthesized fiber-based fillers did not jeopardize the mechanical strength of the experimental adhesives, despite the considerably high concentration ratio used here (20 wt.%). Even though this concentration level was above the typical threshold found in dental adhesives (~ 10 wt.%), the concentration of fillers in contemporary resin adhesives may range from 0.5% to 40% by weight,[66] aiming for both better control of the handling characteristics and increasing the strength properties and film thickness of the adhesive. However, the concentration level of 20 wt.% was chosen in order to obtain a better balance in the content of fibers and availability of DOX released from the DOX-modified adhesive resins. The following calculation was then formulated: considering that the obtained fillers were comprised of ~ 25 wt.% electrospun fibers (measured during preparation of the fillers prior to cryomilling) and the 20 wt.% level used to modify the adhesive resin, it may be presumed that the real fiber content found in each experimental adhesive resin was approximately 5 wt.% in total. Once again, our strategy of using shortened fibers incorporated within the resin matrix of polymeric fillers was not expected to reinforce the resulting material. However, as shown in Figure 7A, the fracture behavior of the fiber-modified adhesives was different from that of the neat unfilled control. Of note, the OS_DOX0% adhesive demonstrated the most non-uniform fracture pattern of the study, showing the roughest topography and the occurrence of multiple planes of fracture. This effect was slightly less evident for the groups containing DOX-loaded fibers, but the latter have still presented an apparently rougher pattern than the control. Noteworthy, the specimens prepared from the unfilled adhesive exhibited a smooth surface, showing typical fractography features, such as mirror, mist area, hackles, and compression curl,[32] which were not clearly observed in the specimens prepared from the fiber-modified adhesives. These fractography features are typical of brittle materials that require less energy consumption during fracture.[67] Conversely, the fiber-modified groups exhibited a rougher surface, which is an indication that the fibers and/or polymeric fillers were stretched during mechanical loading, resulting in detachment/debonding from the resin matrix. Moreover, the creation of cavitations/voids from detachment of the fibers/fillers may alter (reduce) the velocity of crack propagation, thereby increasing energy consumption during fracture.[68] Thus, the presence of the fibrous polymeric fillers seems to positively influence the compliance of resin adhesives, creating frictional and interlocking resistance within the system during loading.[32,69] Despite these findings, and according to the results of the Weibull analysis shown in Figure 7B, all groups demonstrated similar Weibull modulus and characteristic strength values, regardless of the presence of fillers, which confirms the adequate reliability of the experimental adhesives.

Comparing only the fiber-modified groups to each other, we could observe the following trends upon the presence of DOX: flexural strength and hardness reduction; degree of conversion increase; and a slight reduction in hygroscopic and hydrolytic stability, especially for the OS_DOX50% group. We may consider that the tendency toward decreased strength is due to the probable gain in crystalline composition of the DOX-containing adhesives, resulting in a more brittle, less compliant, and less flexible material.[35] Also, the polymeric composition of the DOX0% fillers consists of a mixture of Bis-GMA/HEMA methacrylates, i.e., a typical organic matrix of dental adhesives. Despite being an appropriate resin blend, HEMA possesses a hydroxyl pendant group in its molecular structure, which may favor the

formation of hydrogen bonding, which is attractive in terms of cross-linking and the acquisition of mechanical properties, but also because it is prone to incur hydrolysis, reducing the overall physical stability of the polymer network under wet conditions.[33] One should consider that upon the presence of DOX within the filler carriers, the availability of hydroxyls would be increased, perhaps enhancing susceptibility of the DOX-modified adhesives to hygroscopic and hydrolytic phenomena. Of note, water sorption and solubility were significantly higher within the OS_DOX50% polymer system as compared to the DOX-free counterpart, leading to greater water uptake and the consequent reduction of mechanical properties and the softening effect (plasticizing of the resin matrix).[5] On the other hand, the conversion of monomers was slightly incremented upon the presence of DOX; in this aspect, we may suggest that viscosity, which was apparently greater for the DOX-modified adhesives (data not shown), has played a role. According to Oguri et al.,[70] a minor increase in viscosity may decrease polymer chain termination and reduce mobility of the polymer radicals during the polymerization of resin materials, increasing the free-radical propagation and monomers' conversion (Trommsdorff effect). Gathering together all the present findings on the physico-mechanical performance of the experimental fiber-modified adhesives, the strategy of using DOX-loaded fiber-based fillers shows potential translation to the clinical level, without jeopardizing the overall performance of the control resin adhesive.

3.4. Bonding performance of the fiber-modified adhesives

The outstanding strategy of modifying dental adhesives with filler particles containing DOX-releasing fibers seems to be attractive; however, it should not compromise the bonding performance to dental substrates; otherwise, it would not be feasible for clinical application as a bonding agent. In order to evaluate this outcome, an additional control group was investigated: One-Step® Plus (OS_Plus), a filled version of the OS adhesive resin containing ~ 8.5 wt.% inorganic glass fillers in the resin matrix. From a chemical standpoint, inorganic fillers are usually incorporated into low viscous dental resin adhesives in an attempt to enhance their mechanical performance; an additional goal includes their serving as therapeutic carriers of bioactive agents (e.g., remineralizing ions, antibacterial molecules, MMP inhibitors).[63,71–73] Notwithstanding, the incorporation of inorganic fillers tends to be limited due to their inherent large volume/weight ratio,[63] which differs from polymeric fillers that tend to present a lower surface aspect ratio, thus allowing a greater amount of fillers to be used in the modification of the material. Here, the OS_Plus adhesive was intended to serve as an additional internal control group comprised of reinforcing inorganic fillers on a lower loading level, which differs from our experimental adhesives that consisted of polymeric fillers and upon a greater content (20 wt.%).

As shown in Table 2, the fiber-modified adhesives showed similar immediate bond strengths to dentin as compared to the filled control ($p \geq 0.278$), denoting that the present strategy did not jeopardize the adhesion process to dentin. On the other hand, compared to the unfilled control, the OS_DOX0% group resulted in significantly lower immediate bond strength values ($p < 0.022$). Considering that the same trend was not observed for the DOX-modified materials, we may suggest that something related to the absence of DOX in the DOX0% bonding agent may have reduced its hybridization potential to dentin. Notably, this group exhibited the lowest water sorption of the study, indicating a greater hydrophobic behavior

as compared to the other adhesives, so that a proper chemical interaction between this moderately hydrophobic resin and hydrophilic dentin was probably impaired to some extent. However, the bond strength values were still adequate and befitting with the proper retention of dental restorations. It seems that a proper balance between hydrophilicity and hydrophobicity is an important feature for a resin adhesive to act when forming strong hybrid layers, which indeed corroborates with previous studies.[34,59] One can also consider that the Bis-GMA/HEMA composition of the polymeric fillers has somewhat interacted with the solvent (acetone) and resin monomers' ingredients from the commercial OS adhesive,[33] suggesting that a slight dissolution effect could have occurred within the fillers, which may have also contributed to reduced bonding ability due to chemical instability. However, for the DOX-based fillers, which were probably more crystalline and more cross-linked than the DOX0% fillers (as discussed previously),[48] we may infer that the presence of DOX turned the Bis-GMA/HEMA polymer network to being more chemically stable, guaranteeing an adequate interaction with the resin matrix of the adhesive resin and keeping the bonding ability of the modified material unaltered.

Dental bonds are expected to decrease over time due to the synergistic effects of MMP-mediated collagen degradation and hydrolysis of the adhesive interface.[74] This was truly observed after 12 months of water storage, although with some exceptions. The both control and OS_DOX50% groups demonstrated lower bond strength values ($p \leq 0.035$) after long-term water storage, reducing their adhesion from 19.5% to 25.6%. Conversely, the OS_DOX0% and OS_DOX25% groups presented stable bonds over time ($p \geq 0.389$), with the bond strength reduction ranging from 4.3% to 9.2% only. One may suggest that both hydrolysis and MMP-mediated degradation events were probably diminished within the latter groups, making the dental bonds stable even after the aging simulation used in our study. In terms of hydrolysis prevention, both adhesive resins showed the lowest hydrophilic behavior of the study (i.e., lower water sorption and solubility than the other adhesive resins), decreasing the intensity of hydrolysis and the consequent prevention of fast bond strength degradation.[59] However, in terms of MMP-mediated degradation, only the DOX-modified adhesives could have acted in the inhibition of MMPs/proteases due to the possible release of DOX at both earlier (during adhesive application) and later (during hydrolytic degradation of the hybrid layer) moments. Even though the dental bonds derived from the application of the OS_DOX25% adhesive resulted in the most stable bonds of the study, corroborating the beneficial effects obtained from the release of DOX, the OS_DOX50% group significantly decreased the resin-dentin bonds by 21.7% after aging. This finding confirms that the reduction in bonding performance of dentin bonding agents is a complex condition relying not only on the inactivation of proteases, but also on better control of the hygroscopic and hydrolytic behavior of the materials.[63]

The fracture analysis of dental bonds obtained during immediate testing (24 h) demonstrated a predominance of the adhesive failure mode (Table 2) and, different from the long-term results that showed a greater occurrence of the mixed pattern. Cohesive failures were not frequently observed after long-term water storage, suggesting that an adequate interlocking between bonding agents and dentin was obtained. In this study, nanoleakage was tested to serve as an indirect method to evaluate the quality of the resin-dentin interfaces,[34] and its expression may represent the possible location of defects within the adhesive layer that

would thereafter induce hydrolysis and/or the activation of proteases such as the MMPs tested here. According to the results presented in Figure 8, one should consider that the amount of nanoleakage was similar among the resin-dentin bonds, regardless of the adhesive resin used, implying that the fiber-modified adhesives were adequate as bonding agents. Despite showing a thicker adhesive layer (ca. 3 to 4× thicker), the DOX-modified adhesives resulted in an apparent minimal amount of nanoleakage, with most of the silver nitrate uptake occurring throughout the adhesive layer (white arrows).[75] This finding is important to elucidate that the immediate hybrid layers obtained in this study were adequate, lacking widespread infiltration of residual water molecules. Therefore, any hydrolytic degradation derived from aging of the restoration would be indicative that water uptake occurred, leaving open sites within the adhesive interface for MMP activation and/or breaking of the polymer interactions, which would all impair adhesion. One would consider that the OS_DOX50% and control groups underwent more water uptake and nanoleakage after the long-term period, thus explaining the widest bond strength reduction observed.[76]

One last aspect of this study that needs discussion relies on the authors' choice for using this hybrid mechanism (fiber-containing polymeric fillers) of delivering bioactive agents during application of a dental adhesive system in lieu of the more traditional mechanism that uses inorganic nanoparticles. First, it should be highlighted that while the nanoparticle vehicle tends to result in a burst release process, the nanofiber vehicle works through a drug diffusion mechanism that is typically more controlled and stable over time.[57,62] Therefore, with the present methodology, we tested the combination of both foregoing mechanisms and, based on the findings obtained here, we suggest the release of DOX as an antibacterial agent and potential MMP inhibitor, which was interestingly demonstrated, indicating that stable dental bonds may be acquired with the use of this strategy. No less important, by using the hybrid mechanism described here, we could incorporate a considerably greater amount of fillers (20 wt.%) without jeopardizing the overall performance of the commercial adhesive, i.e., a scenario that is usually challenging when only inorganic carriers are considered. Future studies should focus on the investigation of different bioactive agents (e.g., natural compounds) and polymer sources in the fabrication of fiber-containing polymeric fillers, since this strategy holds potential application in restorative and regenerative dentistry.

4. Conclusion

In the present work, DOX was successfully incorporated into a dental adhesive by using the electrospinning and cryomilling methods, showing a promising application in developing novel bioactive adhesives with MMP inhibition potential and antibacterial activity without jeopardizing important properties and the bonding performance. Remarkably, the resin-dentin bonds were stabilized in the long-term based on the use of fillers comprised of 25 wt.% of the DOX-loaded fibers. Noteworthy, this is the first study reporting on the role of electrospun fibers in the biomodification of a dental adhesive system, thus laying the groundwork for future exploration of nanofibers with therapeutic properties as a strategy to improve the durability of adhesively-bonded resin composite dental restorations.

Acknowledgements

The authors are grateful to Dr. Tatiana dos Santos Ramos and Dr. Josiane Kuhn Rutz for their valuable technical assistance during the bond strength tests performed in the study. This study was financed in part by the Coordenação de Aperfeiçoamento de Pessoal de Nível Superior - Brasil (CAPES) - Finance Code 001 and by grants from the National Institutes of Health (DE026578 and DE023552 to M.C.B.). The content is solely the responsibility of the authors and does not necessarily represent the official views of the National Institutes of Health.

References

1. Tezvergil-Mutluay A, Mutluay M, Seseogullari-Dirihan R, Agee KA, Key WO, Scheffel DL, Breschi L, Mazzoni A, Tjaderhane L, Nishitani Y, Tay FR and Pashley DH, J Dent Res, 2013, 92, 87–91. [PubMed: 23103634]
2. Pashley DH, Tay FR, Breschi L, Tjaderhane L, Carvalho RM, Carrilho M and Tezvergil-Mutluay A, Dent Mater, 2011, 27, 1–16. [PubMed: 21112620]
3. Van Meerbeek B, Yoshihara K, Yoshida Y, Mine A, De Munck J and Van Landuyt KL, Dent Mater, 2011, 27, 17–28. [PubMed: 21109301]
4. Zhang SC and Kern M, Int J Oral Sci, 2009, 1, 163–176. [PubMed: 20690420]
5. Ferracane JL, Dent Mater, 2006, 22, 211–222. [PubMed: 16087225]
6. Fugolin AP, Dobson A, Huynh V, Mbiya W, Navarro O, Franca CM, Logan M, Merritt JL, Ferracane JL and Pfeifer CS, Acta Biomater, 2019.
7. Munchow EA and Bottino MC, Curr Oral Health Rep, 2017, 4, 215–227. [PubMed: 29177123]
8. Gou YP, Meghil MM, Pucci CR, Breschi L, Pashley DH, Cutler CW, Niu LN, Li JY and Tay FR, Acta Biomater, 2018, 75, 171–182. [PubMed: 29883811]
9. Xu R, Yu F, Huang L, Zhou W, Wang Y, Wang F, Sun X, Chang G, Fang M, Zhang L, Li F, Tay F, Niu L and Chen J, Acta Biomater, 2019, 83, 140–152. [PubMed: 30414487]
10. Feitosa SA, Palasuk J, Kamocki K, Geraldeli S, Gregory RL, Platt JA, Windsor LJ and Bottino MC, J Dent Res, 2014, 93, 1270–1276. [PubMed: 25201918]
11. Silva Sousa AB, Vidal CMP, Leme-Kraus AA, Pires-de-Souza FCP and Bedran-Russo AK, Dent Mater, 2016, 32, 1248–1255. [PubMed: 27524231]
12. Acharya MR, Venitz J, Figg WD and Sparreboom A, Drug Resist Updat, 2004, 7, 195–208. [PubMed: 15296861]
13. Nagase H, Visse R and Murphy G, Cardiovasc Res, 2006, 69, 562–573. [PubMed: 16405877]
14. Ryan ME, Greenwald RA and Golub LM, Curr Opin Rheumatol, 1996, 8, 238–247. [PubMed: 8796985]
15. Stanislawczuk R, Reis A and Loguercio AD, J Dent, 2011, 39, 40–47. [PubMed: 20937350]
16. Zhang F, Xia Y, Xu L and Gu N, J Biomed Mater Res B Appl Biomater, 2008, 86, 90–97. [PubMed: 18098184]
17. Akbari V, Jouyandeh M, Paran SMR, Ganjali MR, Abdollahi H, Vahabi H, Ahmadi Z, Formela K, Esmaeili A, Mohaddespour A, Habibzadeh S and Saeb MR, Polymers (Basel), 2020, 12.
18. Porter ML, Munchow EA, Albuquerque MT, Spolnik KJ, Hara AT and Bottino MC, J Endod, 2016, 42, 106–112. [PubMed: 26602451]
19. Bohns FR, Degrazia FW, de Souza Balbinot G, Leitune VCB, Samuel SMW, Garcia-Esparza MA, Sauro S and Collares FM, Sci Rep, 2019, 9, 7710. [PubMed: 31118474]
20. Hamilton MF, Otte AD, Gregory RL, Pinal R, Ferreira-Zandona A and Bottino MC, J Biomed Mater Res B Appl Biomater, 2015, 103, 1560–1568. [PubMed: 25532852]
21. Bottino MC, Thomas V and Janowski GM, Acta Biomater, 2011, 7, 216–224. [PubMed: 20801241]
22. Munchow EA, Albuquerque MT, Zero B, Kamocki K, Piva E, Gregory RL and Bottino MC, Dent Mater, 2015, 31, 1038–1051. [PubMed: 26116414]
23. I. O. f. Standardization, ISO 10993–5, 1993.

24. Bottino MC, Kamocki K, Yassen GH, Platt JA, Vail MM, Ehrlich Y, Spolnik KJ and Gregory RL, J Dent Res, 2013, 92, 963–969. [PubMed: 24056225]
25. Albuquerque MT, Ryan SJ, Munchow EA, Kamocka MM, Gregory RL, Valera MC and Bottino MC, J Endod, 2015, 41, 1337–1343. [PubMed: 25917945]
26. Palasuk J, Kamocki K, Hippenmeyer L, Platt JA, Spolnik KJ, Gregory RL and Bottino MC, J Endod, 2014, 40, 1879–1884. [PubMed: 25201643]
27. Chen JM, Aimes RT, Ward GR, Youngleib GL and Quigley JP, J Biol Chem, 1991, 266, 5113–5121. [PubMed: 1848240]
28. Henn S, de Carvalho RV, Ogliari FA, de Souza AP, Line SR, da Silva AF, Demarco FF, Etges A and Piva E, Clin Oral Investig, 2012, 16, 531–536.
29. Musrati AA, Tervahartiala T, Gursoy M, Kononen E, Fteita D, Sorsa T, Uitto VJ and Gursoy UK, Arch Oral Biol, 2016, 66, 1–7. [PubMed: 26872095]
30. Ferracane JL, Ferracane LL and Braga RR, J Biomed Mater Res B Appl Biomater, 2003, 66, 318–323. [PubMed: 12808590]
31. I. O. f. Standardization, ISO 4049, 2009.
32. Vidotti HA, Manso AP, Leung V, do Valle AL, Ko F and Carvalho RM, Dent Mater, 2015, 31, 1132–1141. [PubMed: 26187528]
33. Munchow EA, Zanchi CH, Ogliari FA, Silva MG, de Oliveira IR and Piva E, J Adhes Dent, 2014, 16, 221–228. [PubMed: 24683593]
34. Cuevas-Suarez CE, Ramos TS, Rodrigues SB, Collares FM, Zanchi CH, Lund RG, da Silva AF and Piva E, Dent Mater, 2019, 35, e204–e219. [PubMed: 31227184]
35. Rosa de Lacerda L, Bossardi M, Silveira Mitterhofer WJ, Galbiatti de Carvalho F, Carlo HL, Piva E and Munchow EA, J Mech Behav Biomed Mater, 2019, 96, 214–218. [PubMed: 31055211]
36. Khalf A and Madihally SV, Mater Sci Eng C Mater Biol Appl, 2017, 76, 161–170. [PubMed: 28482513]
37. Eskitoros-Togay SM, Bulbul YE, Tort S, Demirtas Korkmaz F, Acarturk F and Dilsiz N, Int J Pharm, 2019, 565, 83–94. [PubMed: 31063838]
38. Carvalho LD, Peres BU, Maezono H, Shen Y, Haapasalo M, Jackson J, Carvalho RM and Manso AP, J Appl Oral Sci, 2019, 27, e20180663. [PubMed: 31596368]
39. Bakhsheshi-Rad HR, Hamzah E, Staiger MP, GDias GJ, Hadisi Z, Saheban M and Kashefian M, Materials and Design, 2018, 139, 212–221.
40. Tiyek I, Gunduz A, Yalcinkaya F and Chaloupek J, J Nanosci Nanotechnol, 2019, 19, 7251–7260. [PubMed: 31039883]
41. Wittrig EE, Zablotsky MH, Layman DL and Meffert RM, Implant Dent, 1992, 1, 189–194. [PubMed: 1288813]
42. Trajano VCC, Costa KJR, Lanza CRM, Sinisterra RD and Cortes ME, Mater Sci Eng C Mater Biol Appl, 2016, 64, 370–375. [PubMed: 27127066]
43. Laha A, Sharma CS and Majumdar S, Mater Sci Eng C Mater Biol Appl, 2017, 76, 782–786. [PubMed: 28482590]
44. Boaro LCC, Campos LM, Varca GHC, Dos Santos TMR, Marques PA, Sugii MM, Saldanha NR, Cogo-Muller K, Brandt WC, Braga RR and Parra DF, Dent Mater, 2019, 35, 909–918. [PubMed: 30955856]
45. Eslamian M, Khorrami M, Yi N, Majd S and Abidian MR, J Mater Chem B, 2019, 7, 224–232. [PubMed: 31372224]
46. Meireles AB, Correa DK, da Silveira JV, Millas AL, Bittencourt E, de Brito-Melo GE and Gonzalez-Torres LA, Exp Biol Med (Maywood), 2018, 243, 665–676. [PubMed: 29763386]
47. Guo Z, Wu S, Li H, Li Q, Wu G and Zhou C, Dent Mater J, 2018, 37, 317–324. [PubMed: 29279541]
48. Soskolne WA, Crit Rev Oral Biol Med, 1997, 8, 164–174. [PubMed: 9167091]
49. Dadras Chomachayi M, Solouk A, Akbari S, Sadeghi D, Mirahmadi F and Mirzadeh H, J Biomed Mater Res A, 2018, 106, 1092–1103. [PubMed: 29210169]
50. Chukwudi CU and Good L, J Antibiot (Tokyo), 2019, 72, 225–236. [PubMed: 30737453]

51. Wu Y, Zhou N, Li W, Gu H, Fan Y and Yuan J, Mater Sci Eng C Mater Biol Appl, 2013, 33, 752–757. [PubMed: 25427483]
52. Basrani B and Lemonie C, Aust Endod J, 2005, 31, 48–52. [PubMed: 16128251]
53. Khademi AA, Saleh M, Khabiri M and Jahadi S, J Res Pharm Pract, 2014, 3, 19–22. [PubMed: 24991631]
54. Firestone AR, J Dent Res, 1982, 61, 1243–1244. [PubMed: 6958721]
55. Paes Leme AF, Koo H, Bellato CM, Bedi G and Cury JA, J Dent Res, 2006, 85, 878–887. [PubMed: 16998125]
56. Kumar N and Biswas K, Journal of Materials Research and Technology, 2019, 8, 63–74.
57. Shan X, Liu C, Ouyang C, Gao Q and Zheng K, Designed Monomers and Polymers, 2015, 18, 678–689.
58. Scaffaro R, Maio A, Lopresti F and Botta L, Polymers (Basel), 2017, 9.
59. Breschi L, Maravic T, Cunha SR, Comba A, Cadenaro M, Tjaderhane L, Pashley DH, Tay FR and Mazzoni A, Dent Mater, 2018, 34, 78–96. [PubMed: 29179971]
60. Mazzoni A, Apolonio FM, Saboia VP, Santi S, Angeloni V, Checchi V, Curci R, Di Lenarda R, Tay FR, Pashley DH and Breschi L, J Dent Res, 2014, 93, 263–268. [PubMed: 24334409]
61. Kim HS, Sun X, Lee JH, Kim HW, Fu X and Leong KW, Adv Drug Deliv Rev, 2019, 146, 209–239. [PubMed: 30605737]
62. Ribeiro JS, Daghrery A, Dubey N, Li C, Mei L, Fenno JC, Schwendeman A, Aytac Z and Bottino MC, Biomacromolecules, 2020, 21, 3945–3956.
63. Jun SK, Yang SA, Kim YJ, El-Fiqi A, Mandakhbayar N, Kim DS, Roh J, Sauro S, Kim HW, Lee JH and Lee HH, Sci Rep, 2018, 8, 5663. [PubMed: 29618810]
64. Makela M, Salo T, Uitto VJ and Larjava H, J Dent Res, 1994, 73, 1397–1406. [PubMed: 8083435]
65. Bazrafshan Z and Stylios GK, Int J Biol Macromol, 2019, 129, 693–705. [PubMed: 30769042]
66. Sofan E, Sofan A, Palaia G, Tenore G, Romeo U and Migliau G, Ann Stomatol (Roma), 2017, 8, 1–17. [PubMed: 28736601]
67. Brooks CR and McGill BL, Materials Characterization, 1994, 33, 195–243.
68. Haddadi E, Choupani N and Abbasi F, Engineering Fracture Mechanics, 2016, 162, 112–120.
69. Borges ALS, Munchow EA, de Oliveira Souza AC, Yoshida T, Vallittu PK and Bottino MC, J Mech Behav Biomed Mater, 2015, 48, 134–144. [PubMed: 25933169]
70. Oguri M, Yoshida Y, Yoshihara K, Miyauchi T, Nakamura Y, Shimoda S, Hanabusa M, Momoi Y and Van Meerbeek B, Acta Biomater, 2012, 8, 1928–1934. [PubMed: 22293580]
71. Balbinot GS, Collares FM, Herpich TL, Visioli F, Samuel SMW and Leitune VCB, Dent Mater, 2020, 36, 221–228.
72. Fallahzadeh F, Safarzadeh-Khosroshahi S and Atai M, J Clin Exp Dent, 2017, 9, e738–e742. [PubMed: 28638548]
73. Sauro S, Osorio R, Fulgencio R, Watson TF, Cama G, Thompson I and Toledano M, J Mater Chem B, 2013, 1, 2624–2638. [PubMed: 32260950]
74. Scotti N, Cavalli G, Gagliani M and Breschi L, Int J Esthet Dent, 2017, 12, 524–535. [PubMed: 28983535]
75. Wang X, Song S, Chen L, Stafford CM and Sun J, Acta Biomater, 2018, 74, 326–333. [PubMed: 29751113]
76. Hashimoto M, Yamaguchi S and Imazato S, Current Oral Health Reports, 2015, 2, 195–201.

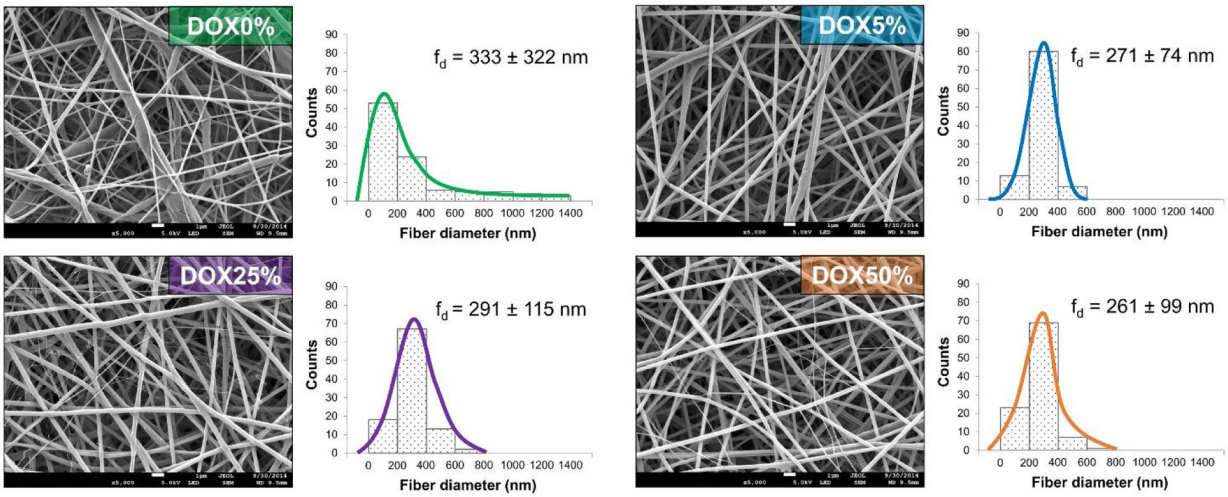

Fig. 1.

Representative SEM micrographs for the different fiber mats obtained via electrospinning and their fiber diameter distribution. f_d: average fiber diameter.

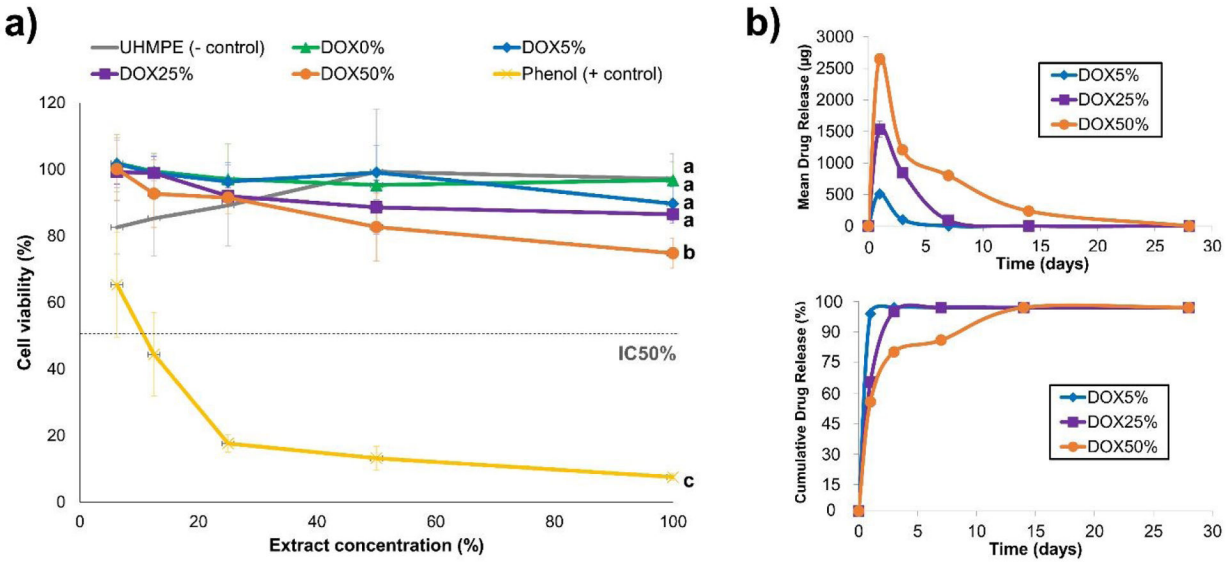

Fig. 2.

Graphs showing the results for cell viability (A) and drug release profile (B) of the fiber mats synthesized in the study. Cytotoxicity assay was performed on each fiber mat group and on the positive (0.3% Phenol) and negative (UHMPE) controls at distinct extract concentrations (6.25%, 12.5%, 25%, 50%, and 100%). Distinct lowercase letters indicate statistically significant differences among the groups at the 100% extract concentration ($p<0.05$); whereas, IC50% indicates the index of cytotoxicity. The graphs on the right show the mean drug release (upper graph) and the cumulative drug release (lower graph) profile of the DOX-loaded fiber mats for up to 28 days of incubation in PBS at 37°C.

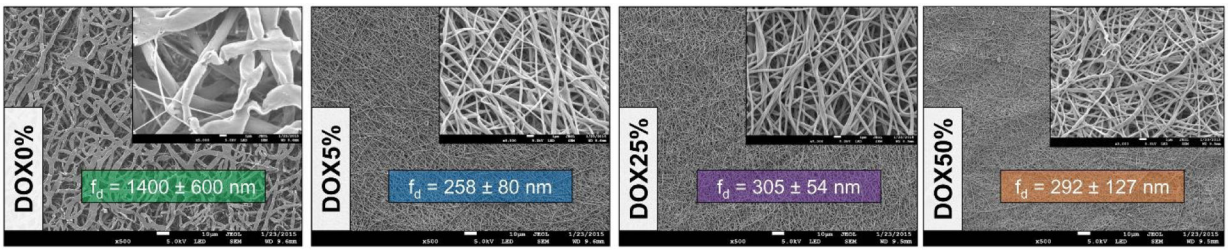

Fig. 3.

Representative SEM micrographs of the fiber mats stored in PBS for 90 days and their respective average fiber diameters (f_d). While the DOX-containing fibers did not seem to alter their morphology and diameter distribution as compared to the baseline, the DOX0% fibers became thicker and acquired a flattened morphology, indicating an intense *in vitro* degradation. Inset micrographs are given at 5,000× magnification.

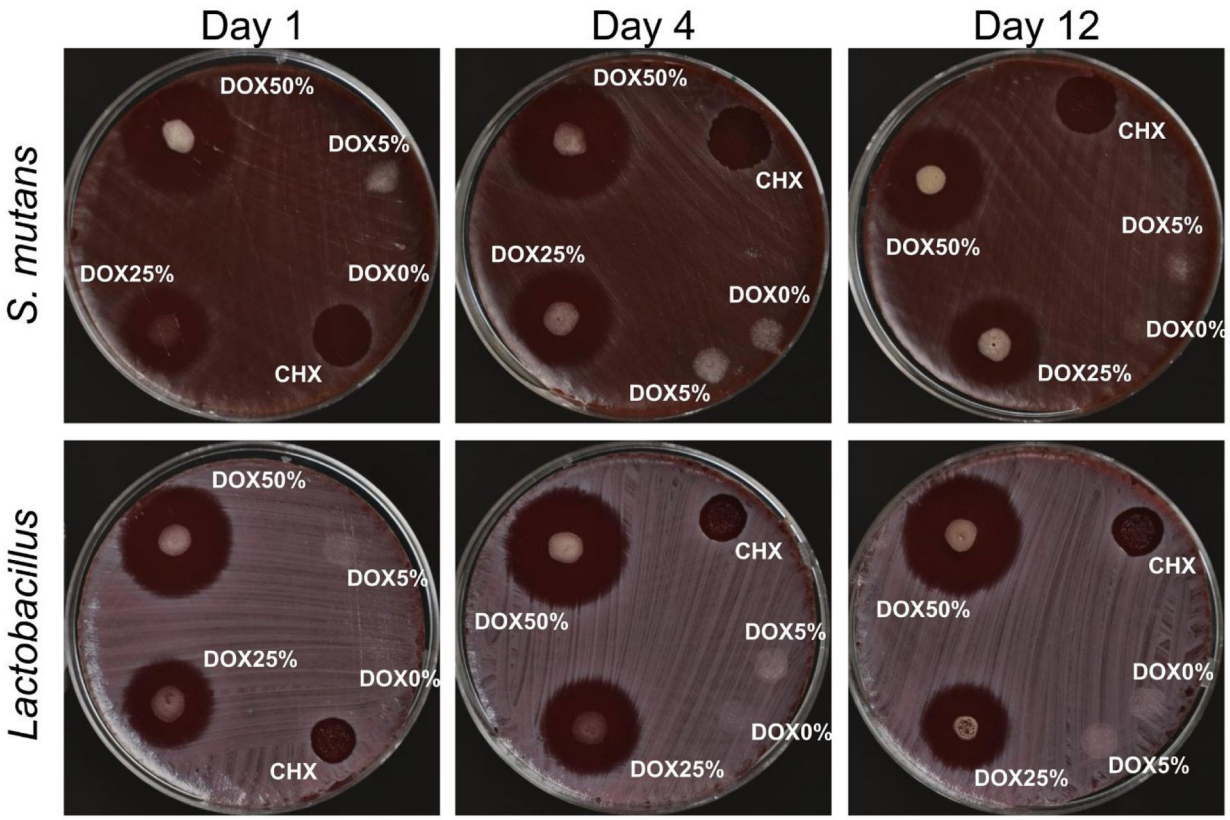

Fig. 4.

Antibacterial activity (inhibition zones) of the DOX-containing fillers against *Streptococcus mutans* and *Lactobacillus* at different incubation periods. The DOX-containing fillers resulted in greater inhibition zones than chlorhexidine (CHX; control), except for the DOX5% fillers, which did not result in any antibacterial activity. The fillers free of DOX (DOX0%) did not demonstrate antibacterial activity against the tested bacteria.

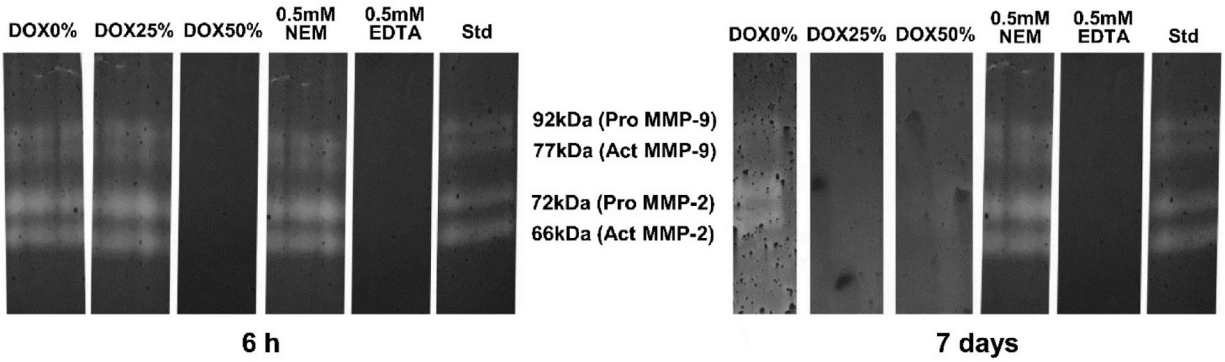

Enzyme assay	Period	DOX0%	DOX25%	DOX50%	0.5mM NEM	0.5mM EDTA	Std (ref.)
92 kDa (Pro MMP-9)	6 h	^{A} 130 ± 1.4 ^{a}	^{A} 131 ± 2.2 ^{a}	^{B} 70 ± 1.2 ^{b}	^{A} 129 ± 1.4 ^{a}	^{A} 71 ± 1.1 ^{b}	100
	7 days	^{B} 122 ± 1.8 ^{a}	^{B} 86 ± 2.0 ^{b}	^{A} 81 ± 0.8 ^{c}	^{B} 122 ± 3.3 ^{a}	^{B} 68 ± 1.2 ^{d}	
77 kDa (Act MMP-9)	6 h	^{A} 127 ± 0.7 ^{a}	^{A} 126 ± 2.5 ^{a}	^{B} 69 ± 0.4 ^{b}	^{A} 125 ± 3.2 ^{a}	^{A} 71 ± 0.9 ^{b}	100
	7 days	^{B} 121 ± 3.1 ^{a}	^{B} 87 ± 4.1 ^{b}	^{A} 80 ± 4.1 ^{b}	^{B} 119 ± 4.5 ^{a}	^{A} 69 ± 2.4 ^{c}	
72 kDa (Pro MMP-2)	6 h	^{A} 158 ± 5.4 ^{a}	^{A} 157 ± 5.3 ^{a}	^{B} 55 ± 1.1 ^{b}	^{A} 159 ± 6.2 ^{a}	^{A} 57 ± 1.5 ^{b}	100
	7 days	^{A} 159 ± 4.7 ^{a}	^{B} 76 ± 1.7 ^{c}	^{A} 70 ± 2.4 ^{c}	^{B} 144 ± 3.3 ^{b}	^{A} 55 ± 0.5 ^{d}	
66 kDa (Act MMP-2)	6 h	^{B} 132 ± 8.3 ^{a}	^{A} 128 ± 4.0 ^{a}	^{B} 43 ± 1.9 ^{b}	^{A} 128 ± 4.2 ^{a}	^{A} 48 ± 2.0 ^{b}	100
	7 days	^{A} 154 ± 1.2 ^{a}	^{B} 84 ± 6.0 ^{c}	^{A} 84 ± 4.5 ^{c}	^{A} 124 ± 2.5 ^{b}	^{A} 48 ± 0.8 ^{d}	

Distinct uppercase and lowercase letters indicate statistically significant differences between groups in the same column (factor "period") and in the same row (factor "eluates"), respectively ($p<0.05$).

Fig. 5.

Gelatin zymography results for the eluates obtained from samples of the DOX0%, DOX25%, and DOX50% fillers after a 6 h and 7-day period. The enzymes were characterized as metalloproteinases, since their expression were inhibited by EDTA (ethylenediaminetetraacetic acid), and NEM (N-ethyl-maleimide) had no effect on enzyme activity. The inset Table shows the results for the percentage increase or reduction (mean ± standard deviation) in the enzymatic activity of latent (Pro) and active (Act) forms of MMP-2 and MMP-9, as compared with Tris–$CaCl_2$ buffer (considered as standard reference; Std), which was taken as 100% of enzyme activity.

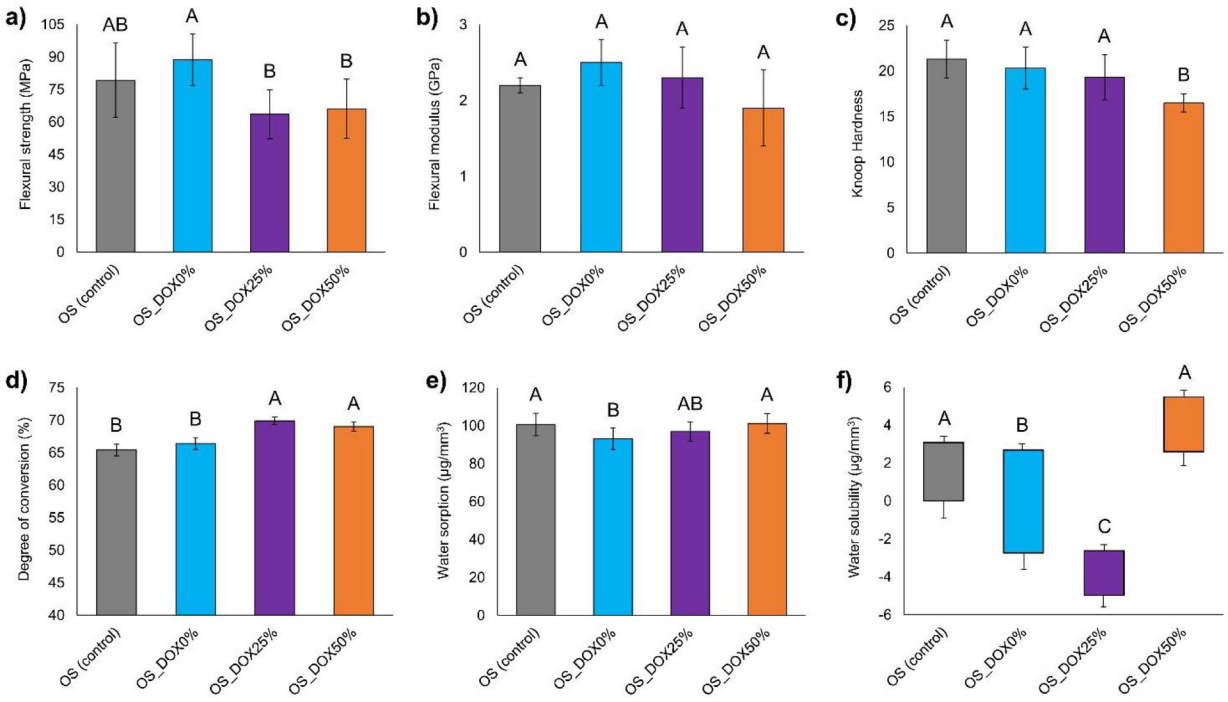

Fig. 6.

Graphs showing the results for flexural strength (A), flexural modulus (B), hardness (C), degree of conversion (D), water sorption (E), and water solubility (F) of fiber-modified adhesives and the unfilled control group. Distinct letters above bars/box plots indicate statistically significant differences among the groups ($p<0.05$; one-way ANOVA for data presented as bars and Kruskal-Wallis for data presented as box plots).

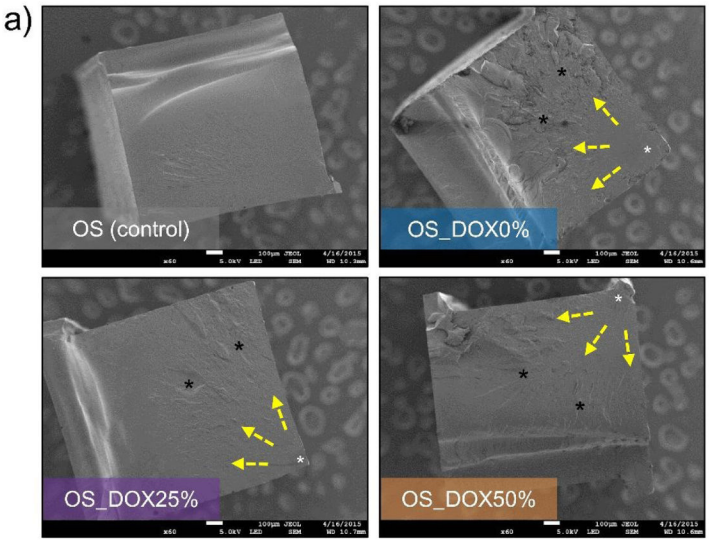

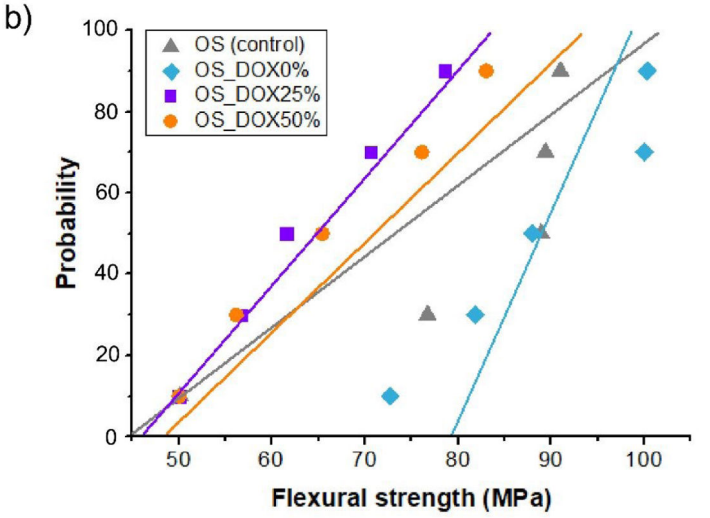

	OS (control)	OS_DOX0%	OS_DOX25%	OS_DOX50%
m	4.3 (1.9 – 7.1) ^{A}	8.4 (3.7 – 14.0) ^{A}	6.6 (2.9 – 10.8) ^{A}	5.6 (2.4 – 9.2) ^{A}
σ_0	89 (75 – 130) ^{AB}	95 (87 – 115) ^{A}	65 (58 – 84) ^{B}	72 (63 – 96) ^{AB}
r^2	0.8430	0.9553	0.9686	0.9626

Fig. 7.

Representative SEM micrographs showing the fractured surfaces of specimens obtained from mechanical characterization of the fiber-modified adhesives and unfilled control (A). While the surface from the control exhibited the smoothest pattern, the surfaces from the fiber-modified groups demonstrated an apparent rougher topography, especially for the OS_DOX0% group, showing the occurrence of typical fractography features, such as mirror (white asterisk), hackles (dashed yellow arrows), mist area (in between mirror and hackles), and compression curl (black asterisk). Graph showing the probability of failure and reliability (inset Table) of the tested groups (B). The results of the Weibull analysis are given as mean (95% confidence intervals) for modulus (m), characteristic strength (σ_0, in MPa),

and coefficient of correlation (r^2) parameters. Distinct letters indicate statistically significant differences among the groups ($p<0.05$).

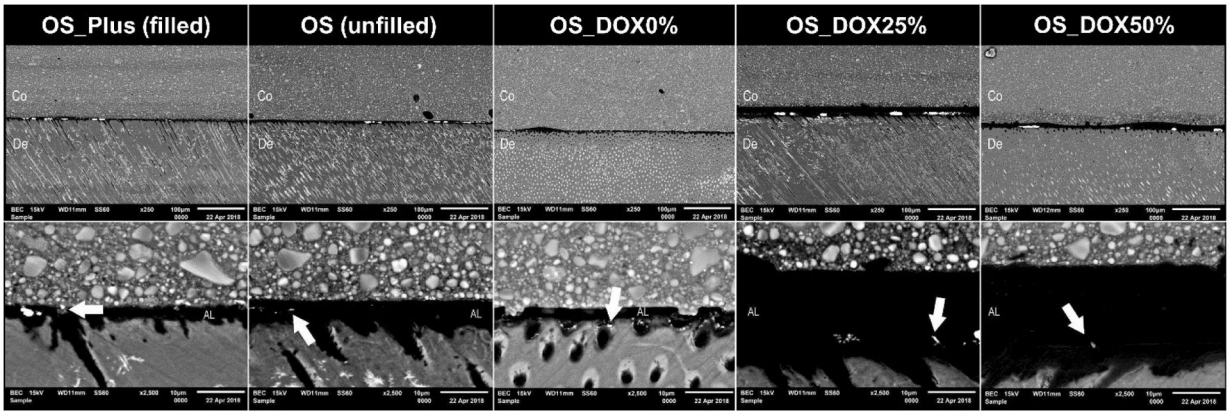

Fig. 8.

Representative SEM micrographs showing the results of nanoleakage for all adhesives tested in the study (commercial controls and the fiber-modified adhesives). Despite the apparent thicker layers for the DOX-modified groups, all hybrid layers demonstrated a similar amount of nanoleakage (white arrows). Co: resin composite; De: dentin; AL: adhesive layer.

Table 1.

Inhibition zones ± standard deviation (in mm) for the DOX-containing fibers and chlorhexidine (CHX, control) against *Streptococcus mutans* and *Lactobacillus*.

Groups	Extract storage in *Streptococcus mutans*				
	Day 1	**Day 3**	**Day 7**	**Day 14**	**Day 28**
DOX5%	9.0 ± 1.0 $^{C, a}$	8.3 ± 0.6 $^{B, a}$	5.7 ± 0.6 $^{B, b}$	0.0 ± 0.0 $^{B, c}$	0.0 ± 0.0 $^{B, c}$
DOX25%	16.0 ± 1.0 $^{B, a}$	13.7 ± 0.6 $^{A, b}$	6.7 ± 0.6 $^{B, c}$	0.0 ± 0.0 $^{B, d}$	0.0 ± 0.0 $^{B, d}$
DOX50%	19.0 ± 1.0 $^{A, a}$	15.7 ± 1.5 $^{A, b}$	8.3 ± 0.6 $^{A, c}$	0.0 ± 0.0 $^{B, d}$	0.0 ± 0.0 $^{B, d}$
CHX	10.0 ± 1.0 $^{C, a}$	10.0 ± 1.0 $^{B, a}$	10.0 ± 1.0 $^{A, a}$	10.0 ± 1.0 $^{A, a}$	10.0 ± 1.0 $^{A, a}$
Groups	**Extract storage in *Lactobacillus***				
	Day 1	**Day 3**	**Day 7**	**Day 14**	**Day 28**
DOX5%	12.0 ± 1.0 $^{B, a}$	10.7 ± 0.6 $^{B, a}$	7.7 ± 0.6 $^{B, b}$	0.0 ± 0.0 $^{B, c}$	0.0 ± 0.0 $^{B, c}$
DOX25%	16.0 ± 1.0 $^{A, a}$	14.7 ± 0.6 $^{A, a}$	9.3 ± 1.5 $^{AB, b}$	0.0 ± 0.0 $^{B, c}$	0.0 ± 0.0 $^{B, c}$
DOX50%	16.3 ± 2.1 $^{A, a}$	9.3 ± 1.5 $^{B, c}$	10.7 ± 1.5 $^{A, b}$	0.0 ± 0.0 $^{B, d}$	0.0 ± 0.0 $^{B, d}$
CHX	12.0 ± 1.0 $^{B, a}$	10.7 ± 1.5 $^{B, a}$	10.7 ± 1.5 $^{A, a}$	8.7 ± 0.6 $^{A, b}$	8.7 ± 0.6 $^{A, b}$

For each bacteria specie tested, distinct superscript uppercase letters in the same column and lowercase letters in the same row indicate statistically significant differences among groups and storage periods tested, respectively ($p<0.05$).

Table 2.

Mean ± standard deviation values for the microtensile bond strength to dentin of the fiber-modified and non-modified (filled and unfilled) adhesives after immediate (24h) and long-term (12 months) water storage, with the respective failure mode distribution (in %).

Groups	Microtensile bond strength (MPa)		Failure modes (24 h)				Failure modes (12 months)			
	24 h	12 months	AD	CD	CR	MI	AD	CD	CR	MI
OS_Plus (filled control)	30.3 ± 5.8 $^{AB, a}$	22.5 ± 4.5 $^{C, b}$	40%	20%	13.3%	26.7%	13.3%	26.7%	20%	40%
OS (unfilled control)	35.9 ± 7.4 $^{A, a}$	28.9 ± 6.4 $^{AB, b}$	26.7%	6.6%	26.7%	40%	20%	0	20%	60%
OS_DOX0%	26.2 ± 5.7 $^{B, a}$	23.8 ± 4.9 $^{BC, a}$	40%	0	13.3%	46.7%	20%	13.3%	0	66.7%
OS_DOX25%	34.9 ± 7.9 $^{A, a}$	33.4 ± 7.1 $^{A, a}$	53.4%	13.3%	13.3%	20%	26.7%	20%	13.3%	40%
OS_DOX50%	34.1 ± 7.8 $^{A, a}$	26.7 ± 5.4 $^{BC, b}$	73.4%	0	6.6%	20%	20%	6.6%	0	73.4%

Distinct uppercase letters indicate statistically significant differences among adhesive groups (at columns), whereas distinct lowercase letters represent statistical differences between periods investigated (at rows); $p<0.05$.

OS_Plus: One-Step® Plus (Bisco); OS: One-Step® (Bisco).

AD: adhesive failure; CD: cohesive failure in dentin; CR: cohesive failure in resin composite; MI: mixed failure.